Supporting Information

A selective Purine-based fluorescent chemosensor for "naked-eye" detection of Zinc ion (Zn^{2+}): applications in live cell imaging and test strips

Haiyan Xu ,[†*a] Wei Chen,[†a] Weixia Zhang,[a] Lixin Ju[a] and Hongfei Lu *[a]

School of Environmental and Chemical Engineering, Jiangsu University of Science and Technology, Zhenjiang, Jiangsu 212003, China

Email: xuhaiyanjurong@163.com, zjluhf1979@just.edu.cn

Table of Contents

1. General information

^{1}H NMR and ^{13}C NMR spectra were recorded on Bruker-Advance DPX 400 MHz spectrometer, using d_6-DMSO as the solvent. The chemical shifts were recorded in ppm. Mass spectra (MS) were performed from Agilent-6110 mass spectrometer. Fluorescent spectra were obtained on Spectrofluorometer FS5. UV–vis spectra were measured using U3010-vis spectrophotometer. The pH levels were carried out with FE20. TLC analysis was performed with Haiyang silica gel F 254 plate and column chromatography was conducted over Haiyang silica gel (type: 200–300 mesh, 300–400 mesh).

All chemical reagents and solvents (analytical grade) were purchased from Energy Chemical and Changhai Wohua Chemical Co. Ltd., and used without further purification. Double distilled water was used through all experiments. Metal salts were obtained from Sinopharm Chemical Co. Ltd., including $AgNO_3$, $CdCl_2$, Cs_2CO_3, $FeCl_3$, $SnCl_2{\cdot}2H_2O$, $CaCl_2$, $FeCl_2{\cdot}4H_2O$, $CuCl_2{\cdot}2H_2O$, $MgCl_2{\cdot}6H_2O$, $CoCl_2{\cdot}6H_2O$, $ZnCl_2$, $Pb(NO_3)_2$, $PdCl_2$, NaCl, $AlCl_3$ and $MnCl_2$.

2. General method for the synthesis of PTAHN

The synthetic methods of probe were summarized in Scheme S1. Probe **PTAHN** was synthesized according to the published procedure.[1-3]

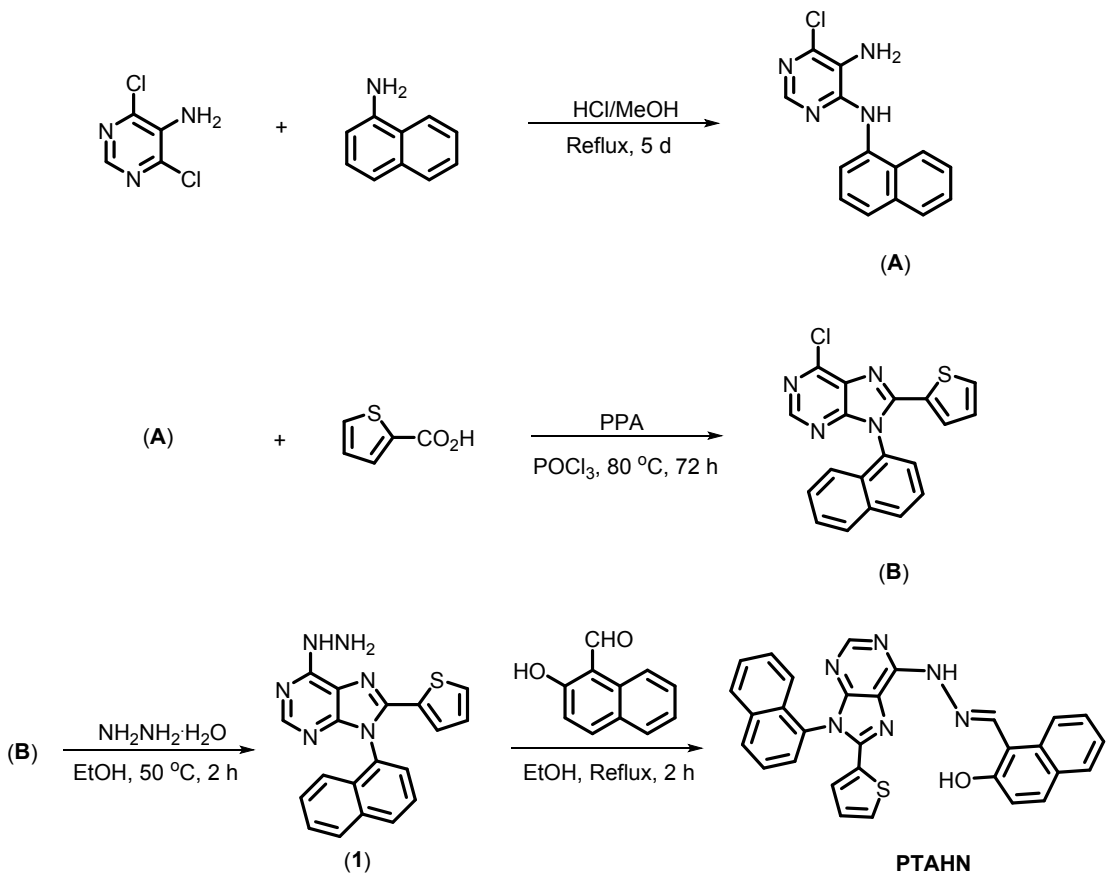

Scheme S1: Synthetic route of **PTAHN**

Synthesis of compound （A）

In a 100 mL round bottom flask, 5-amino-4, 6-dichloropyrimidine (5.00 g, 30 mmol) and 1-naphthylamine (8.58 g, 60 mmol) were added and dissolved in methanol (50 mL), then concentrated HCl (5 mL, 60 mmol) were added. The mixture was stirred at 65 ℃ for 5 d. After cooling to the room temperature, the solvent was evaporated under reduced pressure. And then 1 M NaOH was added, the residue was extracted with ethyl acetate three times. The organic phase was washed with 1.2 M HCl and saturated saline, and then evaporated to obtain the crude produce. The crude product was recrystallized with CH_3OH/H_2O (v/v, 1:5) to afford the compound (**A**)

6-chloro-*N*^{4}-(naphthalen-1-yl)pyrimidine-4,5-diamine (A): Pale violet powder (5.75 g, 71% yield). ^{1}H NMR (400 MHz, DMSO-d_6) δ 8.92 (s, 1H), 7.99 – 7.94 (m, 1H), 7.92 – 7.87 (m, 1H), 7.85 – 7.81 (m, 1H), 7.63 (s, 1H), 7.58 – 7.48 (m, 4H), 5.52 (s, 2H). ^{13}C NMR (100 MHz, DMSO-d_6) δ 151.62, 145.58, 138.88, 135.45, 134.42, 129.88, 128.59, 126.47, 126.33, 126.17, 126.15, 124.96, 123.97, 123.69. ESI-MS m/z:

[M-H]$^-$ calcd. for $C_{14}H_{11}ClN_4$ 269.0, found 269.0.

^{1}H NMR (DMSO)

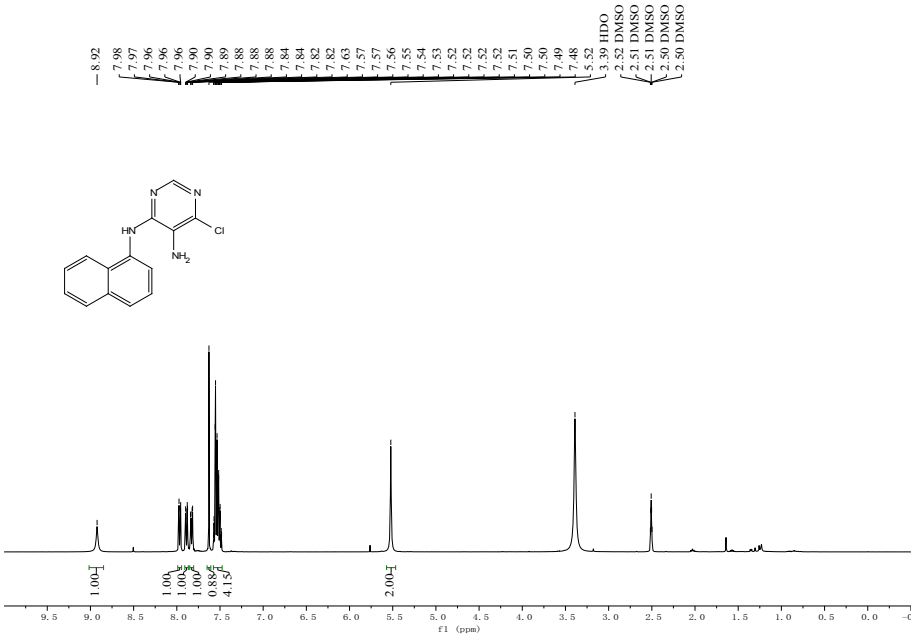

^{13}C NMR (DMSO)

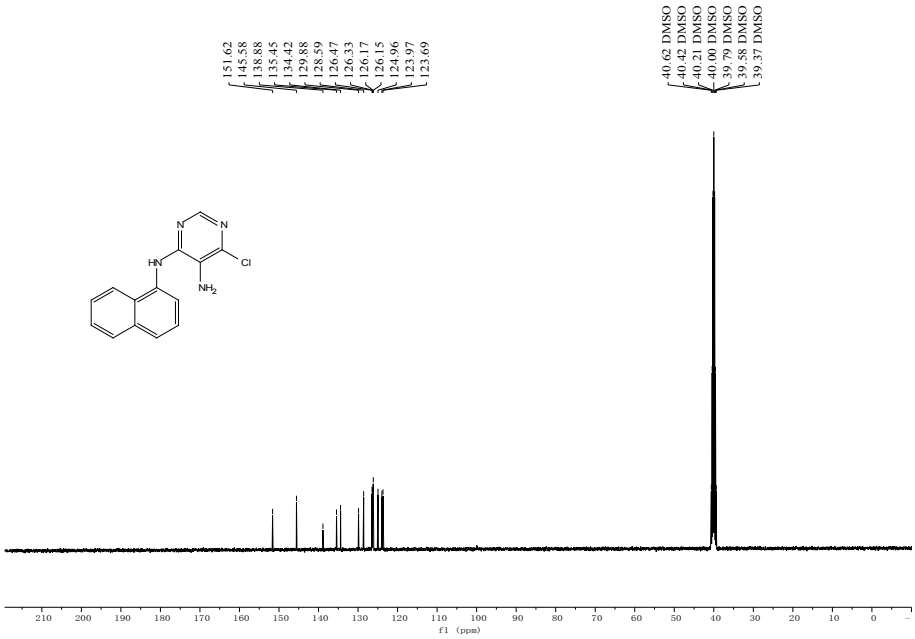

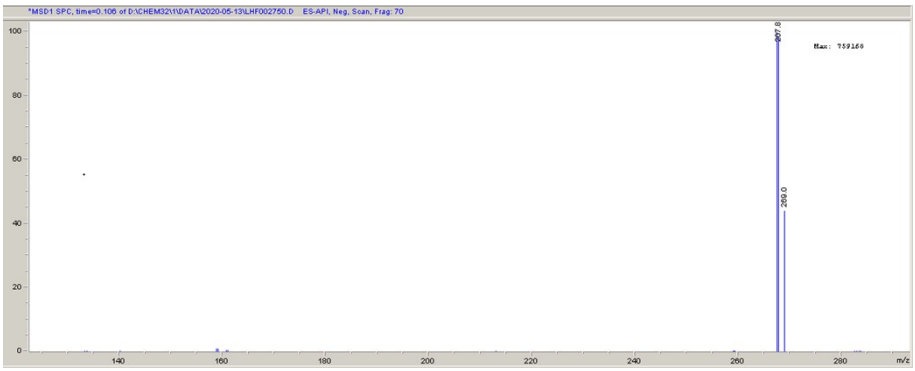

Fig. S1. NMR and MS spectrum of **(A)**

Synthesis of compound （B）

Compound (**A**) (1.00 g, 3.7 mmol), thiophene-2-carboxylic acid (2.37 g, 18.5 mmol), and DTAC (0.10 g, 10 % mmol) were dissolved in 25 mL of $POCl_3$, then PPA (5.00 g, 14.8 mmol) was added. The reaction mixture was stirred at 80 ℃ for 72 h. After the completion of reaction, the solvent was evaporated, and then the residue was purified by column chromatography on silica gel using CH_3OH/CH_2Cl_2 (v/v, 1/250) to afford pure product (B).

6-Chloro-9-(naphthalen-1-yl)-8-(thiophen-2-yl)-9*H*-purine (B): Yellowish solid (0.56 g, 42% yield). ^{1}H NMR (400 MHz, DMSO-d_6) δ 8.62 (s, 1H, H-C=N), 8.34 (d, J = 8.4 Hz, 1H), 8.19 (d, J = 8.2 Hz, 1H), 7.94 – 7.90 (m, 1H), 7.82 – 7.73 (m, 2H), 7.67 – 7.62 (m, 1H), 7.51 – 7.45 (m, 1H), 7.30 (d, J = 9.5 Hz, 1H), 6.98 – 6.94 (m, 1H), 6.85 – 6.81 (m, 1H). ^{13}C NMR (100 MHz, DMSO-d_6) δ 155.70, 152.28, 150.71, 148.35, 134.46, 132.65, 131.73, 130.72, 130.57, 130.54, 130.26, 129.09, 128.77, 128.35, 127.74, 126.50, 122.33. ESI-MS m/z: $[M+H]^+$ calcd. for $C_{19}H_{11}ClN_4S$ 363.0, found 362.9.

^{1}H NMR (DMSO)

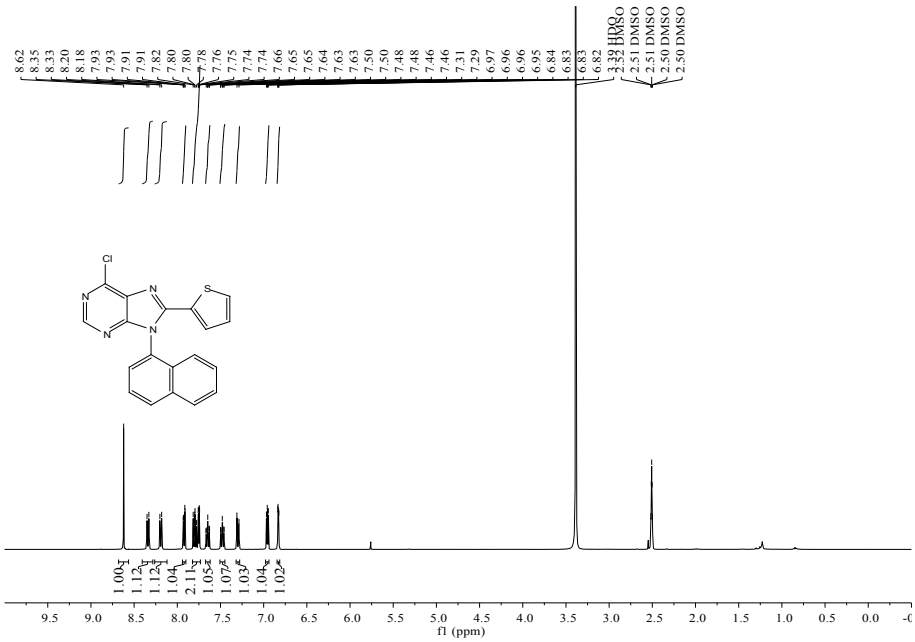
8.62
8.35
8.33
8.20
8.18
7.93
7.93
7.91
7.91
7.82
7.80
7.80
7.78
7.76
7.75
7.74
7.74
7.66
7.65
7.65
7.64
7.63
7.63
7.63
7.50
7.50
7.48
7.48
7.46
7.46
7.31
7.29
6.97
6.96
6.96
6.95
6.84
6.83
6.83
6.82
3.39 HRO
2.52 DMSO
2.51 DMSO
2.51 DMSO
2.50 DMSO
2.50 DMSO
Cl
N
N
N
N
S
1.00
1.12
1.12
1.04
2.11
1.05
1.07
1.03
1.04
1.02
9.5
9.0
8.5
8.0
7.5
7.0
6.5
6.0
5.5
5.0
4.5
4.0
3.5
3.0
2.5
2.0
1.5
1.0
0.5
0.0
f1 (ppm)

^{13}C NMR (DMSO)

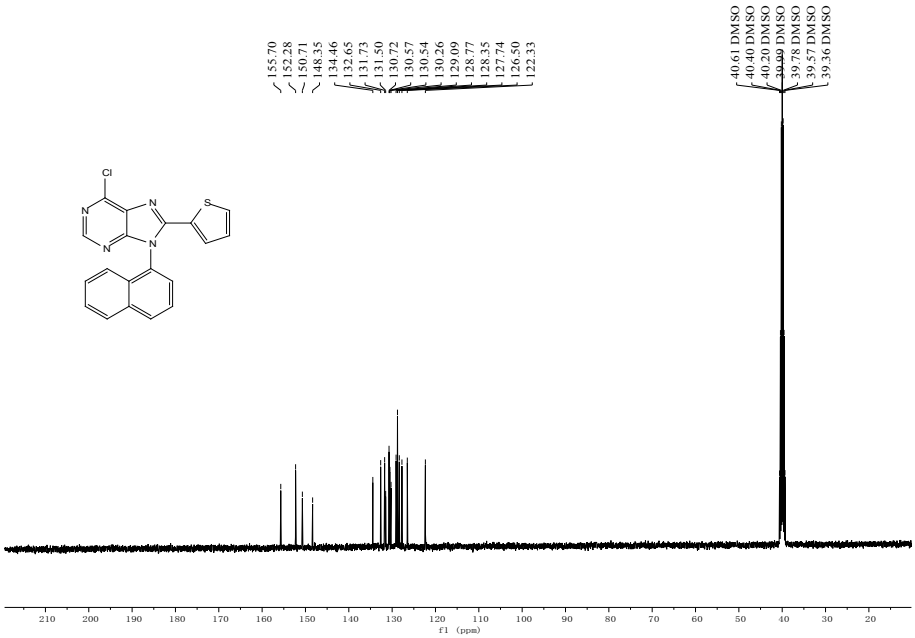
155.70
152.28
150.71
148.35
134.46
132.65
131.73
131.50
130.72
130.57
130.54
130.26
129.09
128.77
128.35
127.74
126.50
122.33
40.61 DMSO
40.40 DMSO
40.20 DMSO
39.99 DMSO
39.78 DMSO
39.57 DMSO
39.36 DMSO
Cl
N
N
N
N
S
210
200
190
180
170
160
150
140
130
120
110
100
90
80
70
60
50
40
30
20
f1 (ppm)

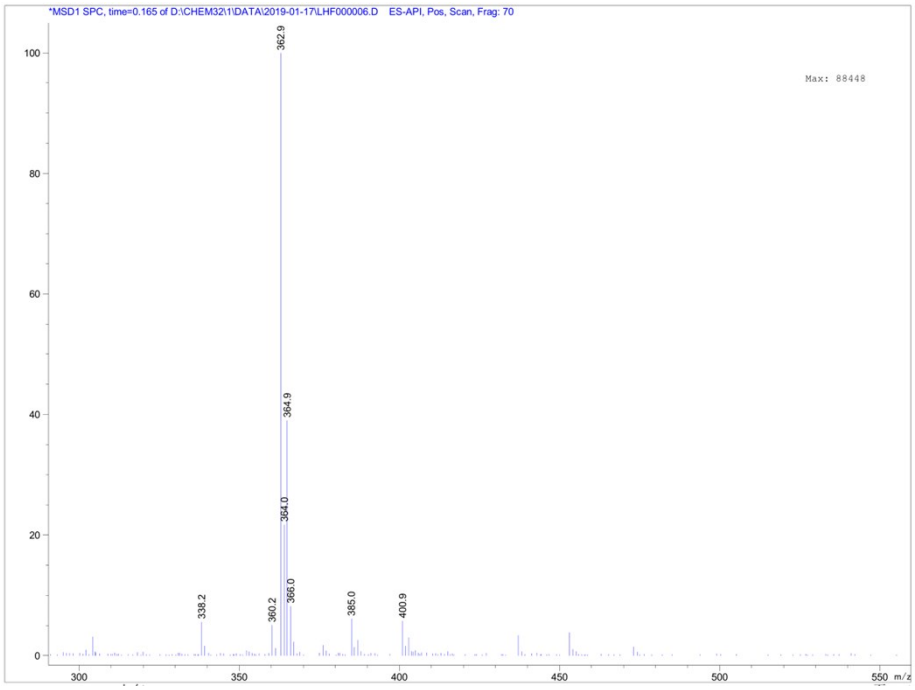

Fig. S2. NMR and MS spectrum of **(B)**

Synthesis of compound （1）

Compound (**B**) (0.29 g, 0.8 mmol) was dissolved in 20 mL of methanol, and then hydrazine was added. The mixture was stirred at 65 ℃ for 3 h. After the reaction completed (monitored by TLC), the reaction mixture was cooled to room temperature. A yellowish powder was collected with filtration, rinsed with MeOH and dried under reduced pressure.

6-Hydrazinyl-9-(naphthalen-1-yl)-8-(thiophen-2-yl)-9*H*-purine (1): Yellowish powder (0.20 g, 70% yield). ^{1}H NMR (400 MHz, DMSO-d_6) δ 9.25 (s, 1H), 8.24 (d, J = 6.9 Hz, 1H), 8.12 (d, J = 6.6 Hz, 1H), 8.06 (s, 1H), 7.76 (d, J = 5.1 Hz, 1H), 7.72 (d, J = 7.0 Hz, 1H), 7.55 (s, 1H), 7.51 (s, 1H), 7.45 – 7.40 (m, 1H), 7.06 – 7.02 (m, 1H), 6.81 (s, 1H), 6.52 (s, 1H), 4.65 (s, 2H). ^{13}C NMR (100 Hz, DMSO-d_6) δ 153.47, 144.60, 134.42, 132.03, 131.54, 131.01, 130.62, 129.69, 129.02, 128.46, 128.21, 128.14, 127.90, 127.49, 126.43, 122.23, 118.09, 79.63. ESI-MS m/z: $[M+H]^+$ calcd.for $C_{19}H_{14}N_6S$ 359.1, found 359.0.

^{1}H NMR (DMSO)

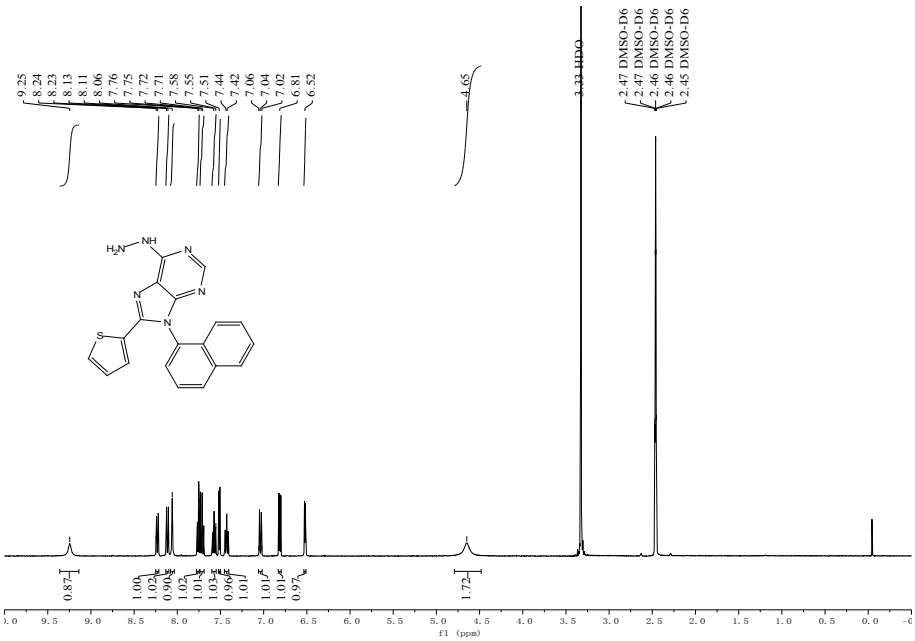
9.25
8.24
8.23
8.13
8.11
8.06
7.76
7.75
7.72
7.71
7.58
7.55
7.51
7.44
7.42
7.06
7.04
7.02
6.81
6.52
4.65
3.33 HDO
2.47 DMSO-D6
2.47 DMSO-D6
2.46 DMSO-D6
2.46 DMSO-D6
2.45 DMSO-D6
0.87
1.00
1.02
0.96
1.02
1.01
1.03
0.96
1.01
1.01
1.01
0.97
1.72
f1 (ppm)

^{13}C NMR (DMSO)

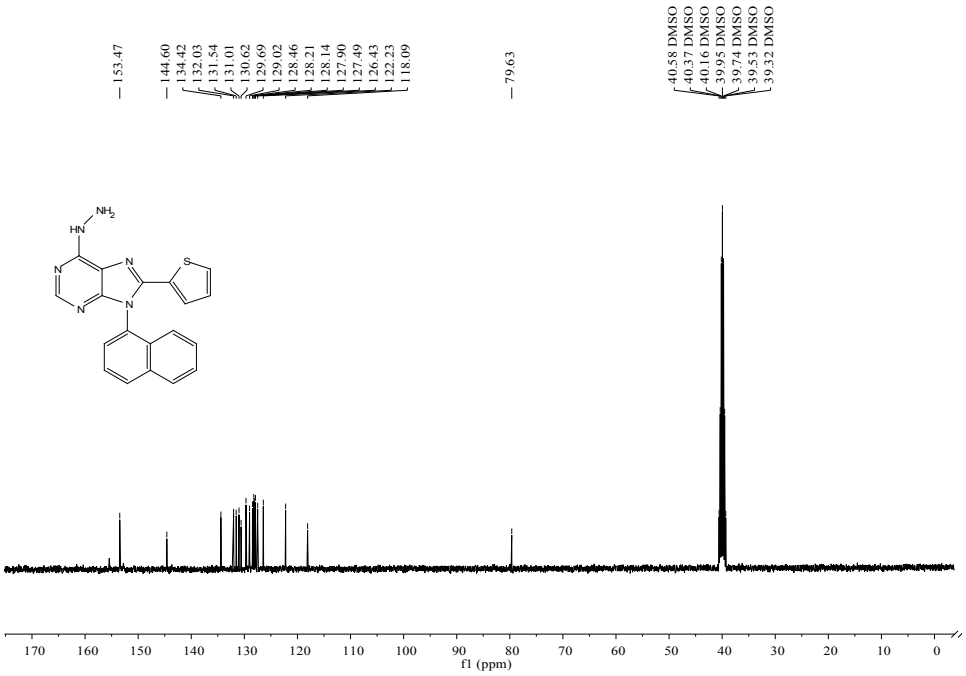
153.47
144.60
134.42
132.03
131.54
131.01
130.62
129.69
129.02
128.46
128.21
128.14
127.90
127.49
126.43
122.23
118.09
79.63
40.58 DMSO
40.37 DMSO
40.16 DMSO
39.95 DMSO
39.74 DMSO
39.53 DMSO
39.32 DMSO
f1 (ppm)

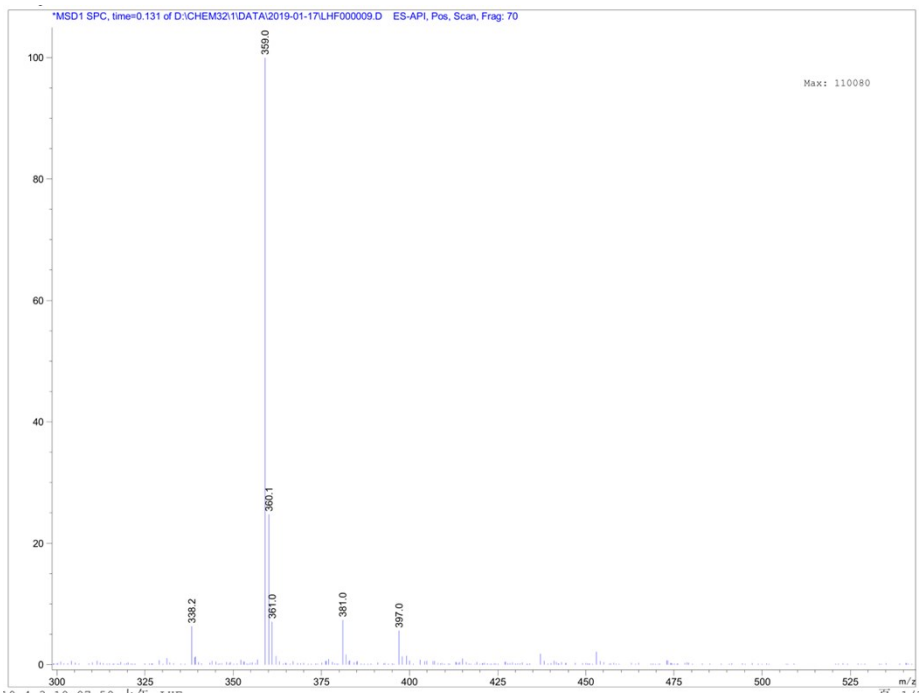

Fig. S3. NMR and MS spectrum of **(1)**

Synthesis of PTAHN

Compound (**1**) (200 mg, 0.558 mmol) and 2-hydroxy-1-naphthaldehyde (144 mg, 0.837 mmol) were dissolved in ethanol (30 mL), and the mixture was refluxed for 2 h. After cooling to room temperature, the solvent was removed under reduced pressure. Then the crude product was purified by recrystallization to produce yellow powder (200 mg, 70%). ^{1}H NMR (400 MHz, DMSO-d_6) δ 12.62 (s, 1H), 12.14 (s, 1H), 9.40 (s, 1H), 8.34 – 8.23 (m, 2H), 8.20 – 8.13 (m, 2H), 7.96 – 7.86 (m, 3H), 7.81 – 7.76 (m, 1H), 7.66 – 7.58 (m, 3H), 7.53 – 7.39 (m, 3H), 7.33 (d, J = 8.9 Hz, 1H), 7.18 (d, J = 9.5 Hz, 1H), 7.02 (s, 1H). ^{13}C NMR (100 MHz, DMSO-d_6) δ 157.16, 152.93, 146.77, 134.50, 132.24, 132.07, 131.31, 131.17, 130.77, 130.68, 129.43, 129.03, 128.56, 128.34, 128.10, 127.97, 127.53, 126.45, 123.86, 122.33, 120.68, 119.98, 118.93, 109.31. ESI-MS m/z: $[M+H]^+$ calcd for $C_{30}H_{21}N_6OS$ 513.1, found 513.0.

^{1}H NMR (DMSO)

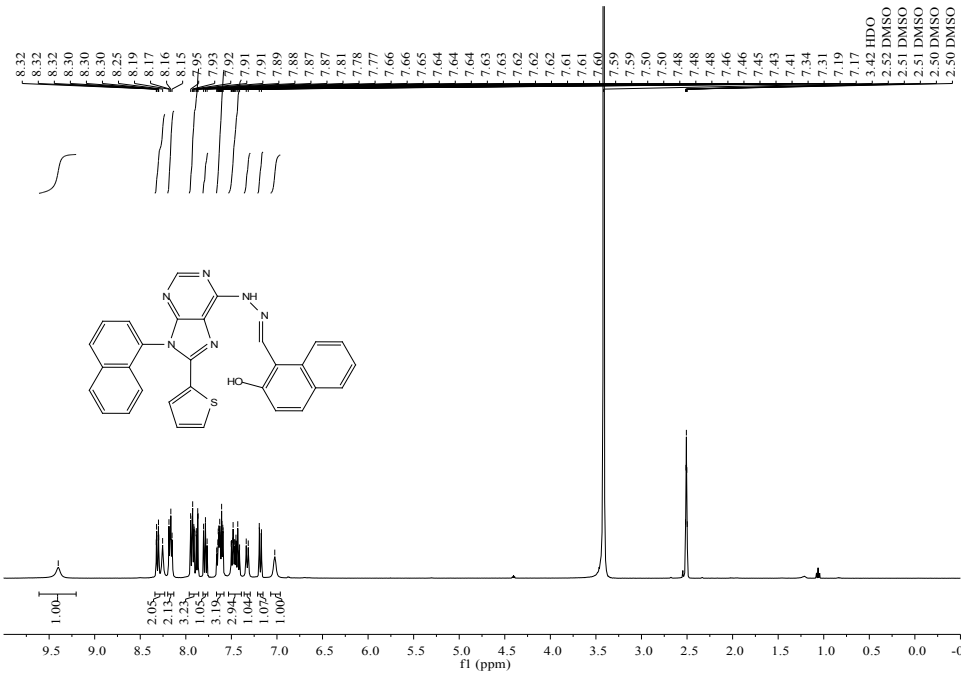
8.32
8.32
8.32
8.30
8.30
8.30
8.25
8.19
8.17
8.16
8.15
7.95
7.93
7.92
7.91
7.91
7.89
7.88
7.87
7.87
7.81
7.78
7.77
7.66
7.66
7.65
7.64
7.64
7.64
7.63
7.63
7.62
7.62
7.62
7.62
7.61
7.61
7.60
7.59
7.59
7.59
7.50
7.50
7.48
7.48
7.48
7.46
7.46
7.45
7.43
7.41
7.34
7.31
7.19
7.17
3.42 HDO
2.52 DMSO
2.51 DMSO
2.51 DMSO
2.50 DMSO
2.50 DMSO
N
N
NH
N
N
N
HO
S
1.00
2.05
2.13
3.23
1.05
3.19
2.94
1.04
1.07
1.00
9.5
9.0
8.5
8.0
7.5
7.0
6.5
6.0
5.5
5.0
4.5
4.0
3.5
3.0
2.5
2.0
1.5
1.0
0.5
0.0
f1 (ppm)

^{13}C NMR (DMSO)

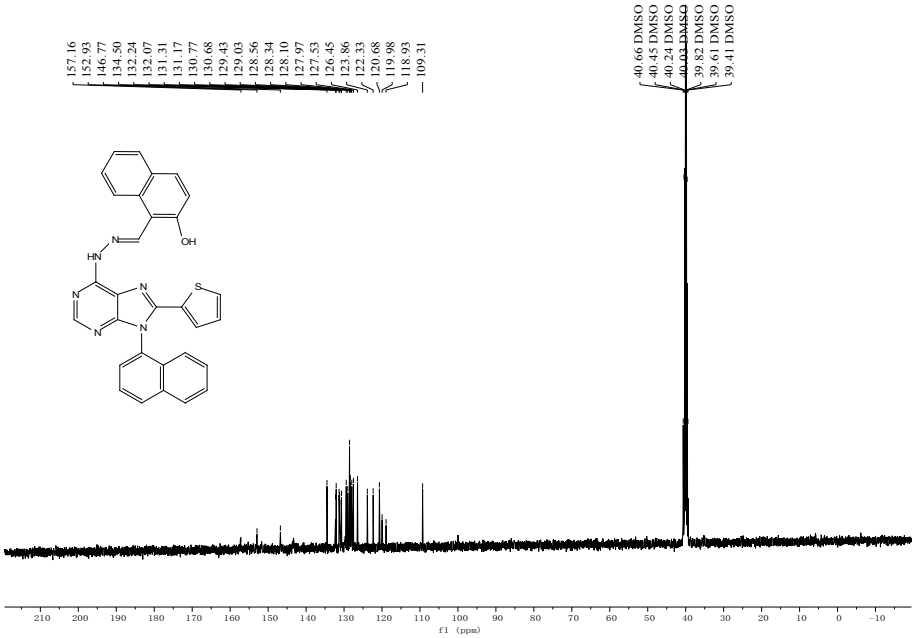
157.16
152.93
146.77
134.50
132.24
132.07
131.31
131.17
130.77
130.68
129.43
129.03
128.56
128.34
128.10
127.97
127.53
126.45
123.86
122.33
120.68
119.98
118.93
109.31
40.66 DMSO
40.45 DMSO
40.24 DMSO
40.03 DMSO
39.82 DMSO
39.61 DMSO
39.41 DMSO
N
OH
HN
N
N
N
S
210
200
190
180
170
160
150
140
130
120
110
100
90
80
70
60
50
40
30
20
10
0
−10
f1 (ppm)

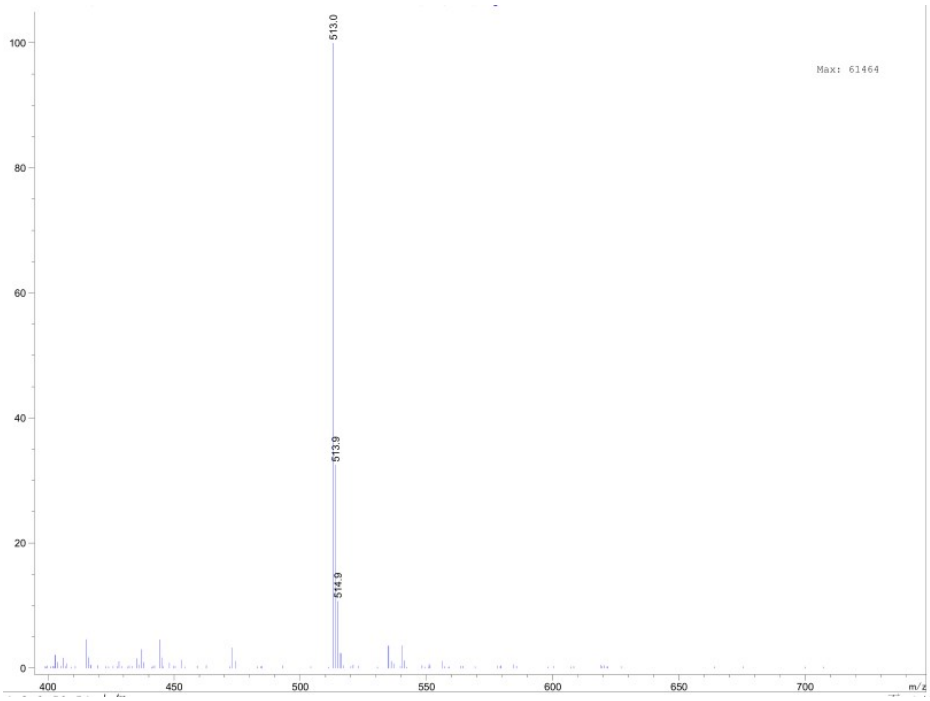

Fig. S4. NMR and MS spectrum of **PTAHN**

3. Binding association constant

The limit of detection (LOD) of **PTAHN** for Zn^{2+} was determined from the following equation: LOD = 3Sb1/S, Sb1 is the standard deviation of the blank solution; S is the slope of the calibration curve. From the Fig. S5 we get the slope (S) = 30053.57143, Standard deviation Sb1 = 616.8737. Thus, using the formula we get the LOD = 61.6 nM.

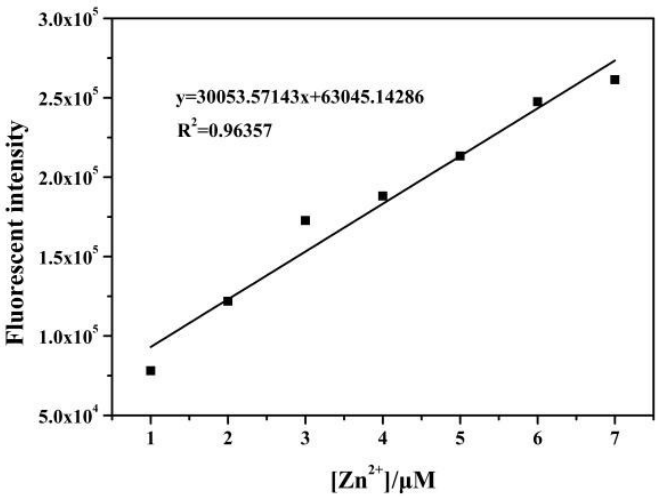

Fig. S5. Calibration curve for fluorescence titration of **PTAHN** with Zn^{2+}

The association constant of **PTAHN**-Zn^{2+} complex was determined as

1.566×10^5 M^{-1} on the basis of Benesi-Hilderband equation (Fig. S6).

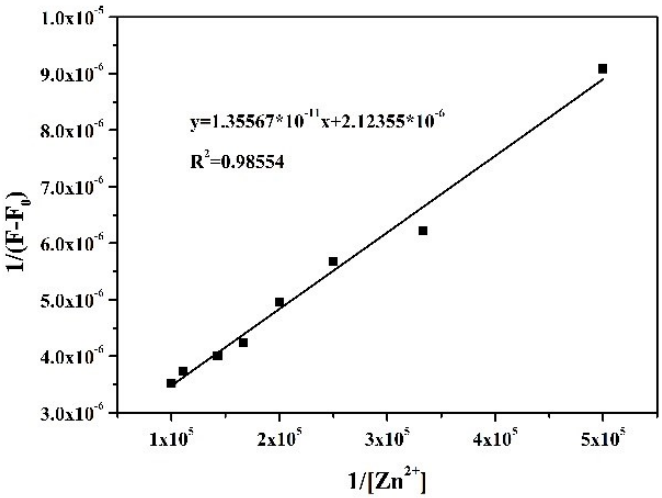

Fig. S6. Benesi-Hildebrand plot of **PTAHN** using 1:1 stoichiometry for association between **PTAHN** and Zn^{2+} ion.

4. Spectroscopic responses of PTAHN-Zn^{2+} towards anions

In addition to the properties of **PTAHN** for recognition of cations, the **PTAHN-Zn^{2+}** complex was also applied as a metal-based sensor for detecting anions. Various anions (50 μM), such as F^-, NO_2^-, CH_3COO^-, $S_2O_3^{2-}$, SO_4^{2-}, HPO_4^{2-}, SO_3^{2-}, HS^-, CO_3^{2-}, $H_2PO_4^-$, HSO_3^-, S^{2-}, NO_2^-, I^-, HCO_3^-, and Br^-, was tested for their interfering effects in the fluorescence spectrum of **PTAHN-**Zn^{2+} complex (50 μM). As shown in Fig. S7, the aforementioned anions induced almost negligible fluorescence changes. However, upon the addition of EDTA to the solution of **PTAHN-**Zn^{2+}, the fluorescence intensity was reduced immediately, which could be ascribed to the removal of Zn^{2+} by EDTA.

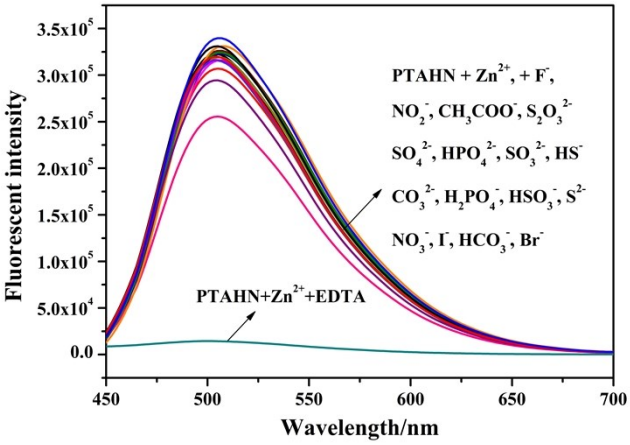

Fig. S7. Fluorescent spectra of **PTAHN-**Zn^{2+} with the addition of various anions in in DMSO/H_2O solution (9/1, v/v, pH 7.4, HEPES buffer, 0.2 mM)

5. Solvent screening

The solvent effect on the fluorescence intensity of **PTAHN-**Zn^{2+} was also investigated. The solvents, including DMSO, THF, acetone, EtOH, MeOH, and CH_3CN were selected to prepare **PTAHN** solution (10 μM). Then upon the addition of Zn^{2+} (50 μM, 5 equiv) to each **PTAHN** solution, the fluorescence emission intensity was tested in the same manner. As displayed in Fig. S8, DMSO was found as the optimized solvent for the enhanced fluorescence emission intensity of **PTAHN-**Zn^{2+} at 501 nm.

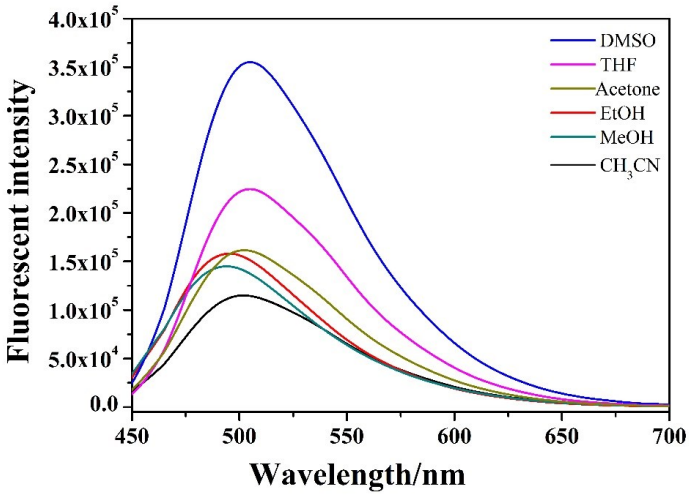

Fig. S8. The solvent effect of the fluorescence intensity of **PTAHN-**Zn^{2+} complex

6. ^{1}H NMR titration experiments

To better explore binding mode of **PTAHN** with Zn^{2+} ion, ^{1}H NMR spectra of probe **PTAHN** with Zn^{2+} ion were performed in DMSO-d_6. When 1.0 and 5.0 equiv. Zn^{2+} ion was separately added to **PTAHN,** the –OH signal at 12.60 was shifted to 13.02 ppm and the HC=N signal at δ 9.37 ppm unfiled shifted to 9.63 ppm. At the same time, the proton of pyrimidine ring at 8.25 downfield shifted to 8.23 ppm, which support the notion that the pyrimidine nitrogen atom participated in binding with Zn^{2+} ion.

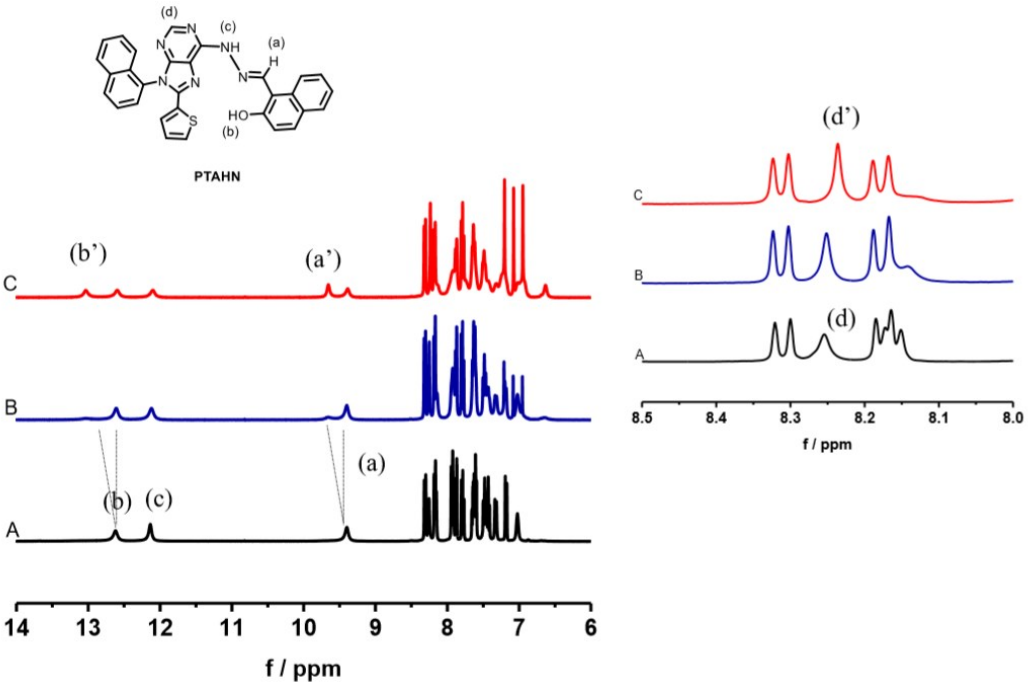

Fig. S9. ^{1}H NMR spectra of (A) **PTAHN** in the presence of (B) 1.0, (C) 5.0, equiv. of Zn^{2+} in DMSO-d_6.

7. The response rate of PTAHN towards Zn^{2+} ion

The response rate of **PTAHN** towards Zn^{2+} has been investigated. As the figure shown below, the response time of **PTAHN** towards Zn^{2+} depends on the concentration of Zn^{2+} ion. The response time of **PTAHN** towards Zn^{2+} reduced with the incremental addition of the concentration

of Zn^{2+} ion. According to the Fig. S10 (b), the pseudo-first order rate constant was determined to be 0.26565 min^{-1}.

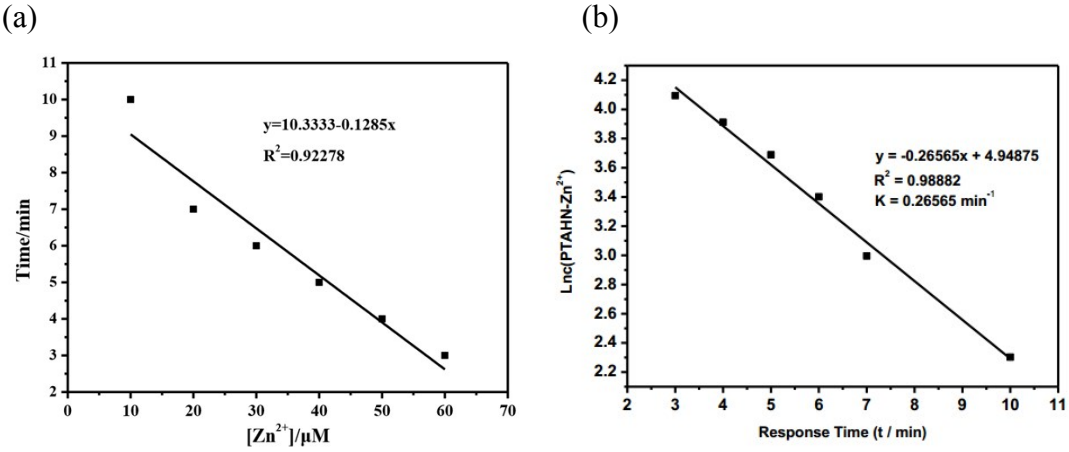

Fig. S10. (a) The response rate of **PTAHN** towards different concentrations of Zn^{2+} ion; (b) Lnc(**PTAHN**-Zn^{2+}) towards response time (min)

8. Comparison with recently reported probes

Some comparison of reported fluorescence probes for the detection of Zn^{2+} ions based on Schiff base were listed in Table S1, probe **PTAHN** exhibited some advantages while few parameters of other probes were better than this work. First, probe **PTAHN** displayed a "turn-on" fluorescence response towards Zn^{2+} ion in 30s and with an obvious color change from the colorless to yellow. Besides, the LOD value of probe **PTAHN** towards Zn^{2+} appeared sensitivity in the nM level while few probes in this table showed LOD values in this range, which indicated high sensitivity of **PTAHN** towards the Zn^{2+} ion. Importantly, it was the beneficial characteristics that our probe could be successfully used for imaging the intracellular Zn^{2+} in living cells, as well as monitoring Zn^{2+} in the solid state.

Table S1. Some comparison of reported fluorescence probes for Zn^{2+} ion

Chemical structure	Ex/Em	LOD	Solvent	Application	Ref.

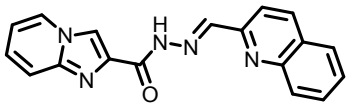	375/462	68 nm	C_2H_5OH-H_2O (9:1)	Not mentioned	4
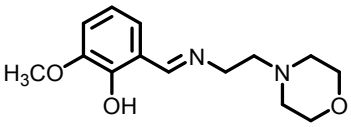	340/490	40.5 nm	Water-methanol (1:9)	living cells	5
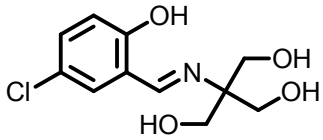	370/458	4.9 nm	Tis–HCl buffer solution	living cells	6
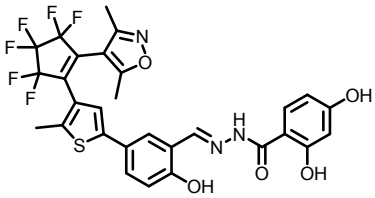		1.28 μM	THF	logic circuit	7
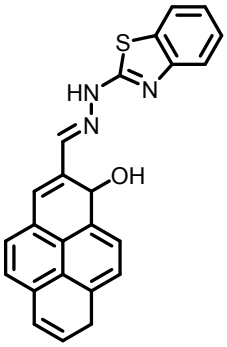	386/526	0.258 μM	EtOH-HEPES buffer (65:35)	living cells	8
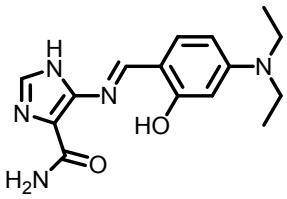	420/484	1.59 μM	Bis–Tris buffer–DMF solution (997:3)	living cells	9
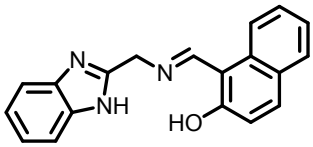	375/447	2.26 μM	Bis-tris buffer	living cells	10
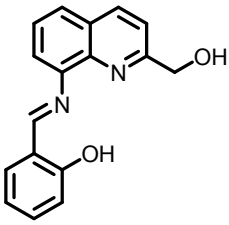	416/530	11.5 nm	EtOH-H_2O solution (v/v=4/1)	living cells; Paper test	11

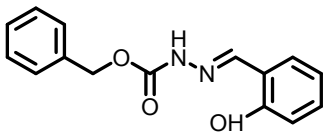	280/452	1.12 μM	aqueous media	living cells	12
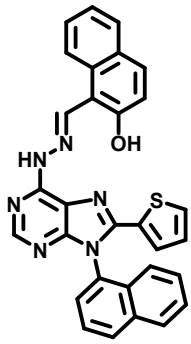	422/501	61.6 nm	DMSO/H_2O solution (9/1)	living cells; Paper test	This work

9. Cytotoxicity test

The cytotoxicity of **PTAHN** against to the HepG2 cells was measured by MTT assay (Fig. S11). HepG2 cells were seeded into a 96-well plate at a density of about 7000 cells per well. After the cells were attached at 37 ^{o}C under a humidified atmosphere of 5% CO_2 in air, 100 μL fresh culture medium with different PTAHN concentrations (0, 2, 4, 6, 8, 10, 12, 14, 16 and 18 μM) were added and incubated for 24 h. Subsequently, 10 μL MTT reagent was added into each well and incubated for another 3 h. As seen in Figure S11, 10 μM of probe **PTAHN** had no obvious effect on HepG2 cells growth after 24 h.

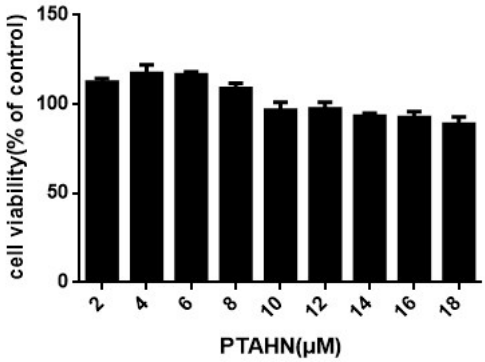

Fig. S11. Cytotoxic effect of probe **PTAHN** on HepG2 cells. Cells were treated with different **PTAHN** concentrations and its survivability was measured by MTT assay

10. DFT Calculation

Geometry optimization of **PTAHN** and **PTAHN**-Zn^{2+} complex were performed by DFT/B3LYP method using Gaussian 09 software.[13-14] lanl2dz basis set was applied to Zn^{2+} while 6-31+g(d) basis set was used to other elements (C, O, H, N，S). Vibrational frequency calculations were performed to confirm that all structures were at the local minima (the number of the imaginary frequency is zero) on the potential surfaces.

11. References

1. X. Jin, H. Chen, W. Zhang, B. Wang, W. Shen and H. Lu, *Appl Organometal Chem.,* 2018, **32,** 1−9.
2. W. Zhang, X. Jin, W. Chen, C. Jiang, and H. Lu, *Anal. Methods*, 2019, **11**, 2396−2403.
3. G. Wu, Z. Wang, W. Zhang, W. Chen, X. Jin and H. Lu, *Inorg. Chem. Commun.*, 2019, **102**, 233−239.
4. S. Xiao, Z. Liu, J. Zhao, M. Pei, G. Zhang and W. He, *RSC Adv.*, 2016, **6**, 27119–27125.
5. K. Ghosh, S. Dey, S. Halder, A. Bhattacharjee, C. Rizzoli and P. Roy, *J. Mol. Struct.*, 2016, **1118**, 325–334.
6. L. Yan, R. Li, F. Ma and Z. Qi, *Anal. Methods*, 2017, ***9***, 1119–1124.
7. Z. Shi, Y. Tu and S. Pu*, RSC Adv.,* 2018, **8**, 6727–6732.
8. Y. Tang, Y. Huang, L. Lu, C. Wang, T. Sun, J. Zhu, G. Zhu, J. Pan, Y. Jin, A. Liu and M. Wang, *Tetrahedron lett.*, 2018, **18**, 31128–31134.
9. J. Y. Yun, J. B. Chae, M. Kim, M. H. Lim and C. Kim, *Photochem. Photobiol. Sci.*, 2019, **18**, 166–176.
10. J. Y. Yun, A. Kim, S. M. Hwang, D. Yun, H. Lee, K. –T. Kim and C. Kim, *Bull. Chem. Soc. Jpn.,* 2019, **92**, 961–966.
11. J. Fu, Y. Chang, B. Li, H. Mei, L. Yang and K. Xu, *Analyst*, 2019，**144**，5706–5716.
12. S. Kim, H. Lee, H. So, H. Lee, K. - T. Kim and C. Kim. *Spectrochim. Acta A*, 2019, **228**, 117787.

13. M. J. Frisch, G. W. Trucks, H. B. Schlegel, G. E. Scuseria, M. A. Robb, J. R. Cheeseman, G. Scalmani, V. Barone, B. Mennucci, G. A. Petersson, H. Nakatsuji, M. Caricato, X. Li, H. P. Hratchian, A. F. Izmaylov, J. Bloino, G. Zheng, J. L. Sonnenberg, M. Hada, M. Ehara, K. Toyota, R. Fukuda, J. Hasegawa, M. Ishida, T. Nakajima, Y. Honda, O. Kitao, H. Nakai, T. Vreven, J. A. Montgomery, Jr., J. E. Peralta, F. Ogliaro, M. Bearpark, J. J. Heyd, E. Brothers, K. N. Kudin, V. N. Staroverov, R. Kobayashi, J. Normand, K. Raghavachari, A. Rendell, J. C. Burant, S. S. Iyengar, J. Tomasi, M. Cossi, N. Rega, J. M. Millam, M. Klene, J. E. Knox, J. B. Cross, V. Bakken, C. Adamo, J. Jaramillo, R. Gomperts, R. E. Stratmann, O. Yazyev, A. J. Austin, R. Cammi, C. Pomelli, J. W. Ochterski, R. L. Martin, K. Morokuma, V. G. Zakrzewski, G. A. Voth, P. Salvador, Gaussian 09, Revision D.01, Gaussian Inc., Wallingford., 2013.
14. A. D. Becke, J. Chem. Phys., 1993, 98, 5648–5652.